Quantum Dots II

1. Open Dot Experiments
2. Kondo effect
3. Few Electron Dots
4. Double Quantum Dots

Huibers, Ph.D. Thesis (1999)
Huibers et al., PRL83, 5090 (1999)

Open Dot Regime

Open Dot

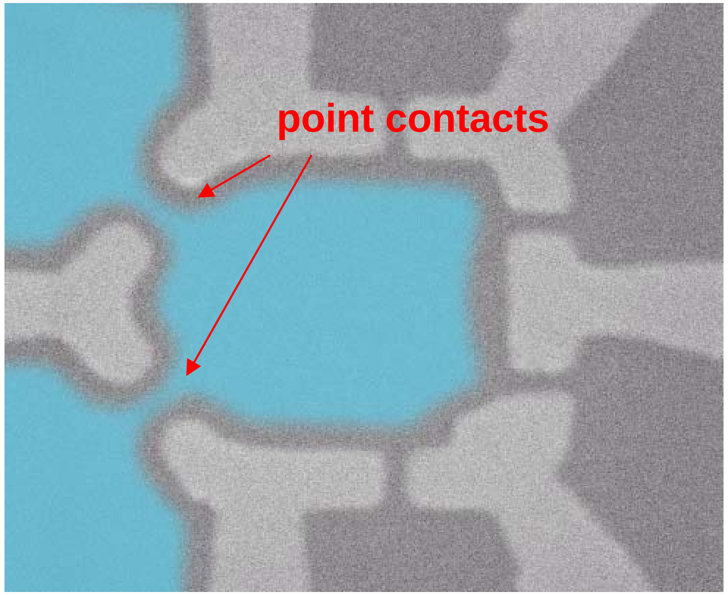

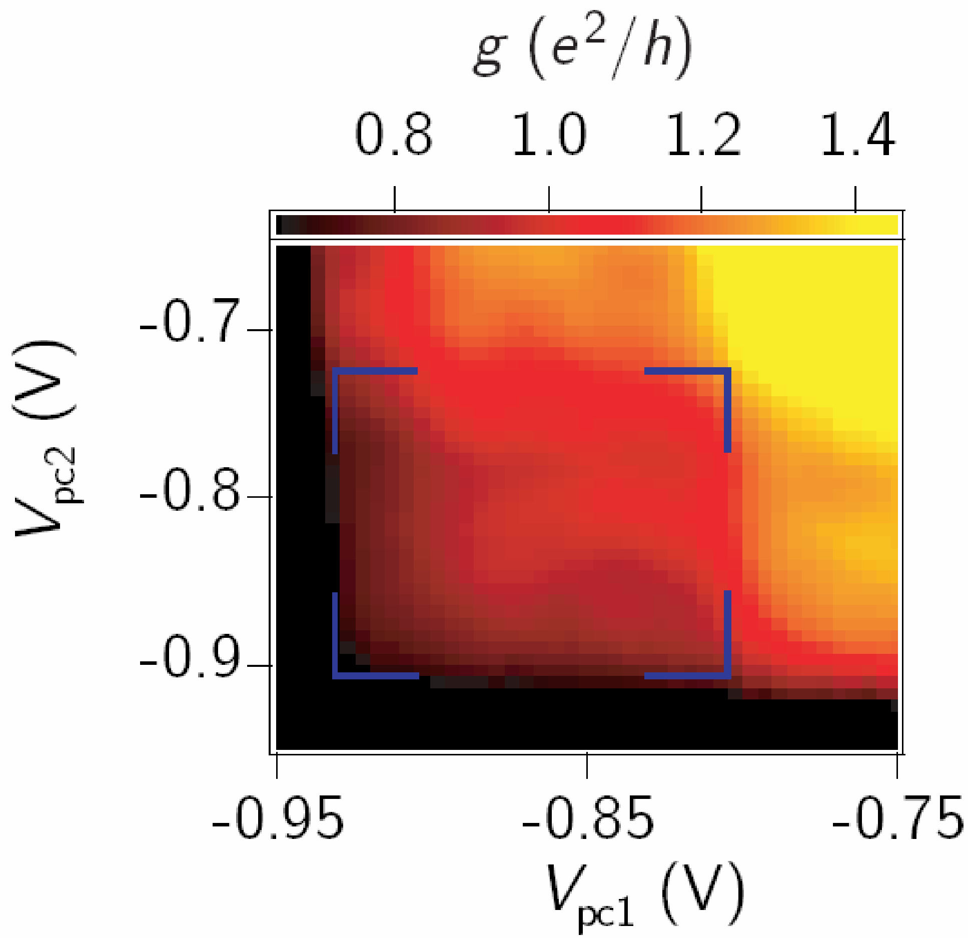

- V_{gate} set to allow ≥ $2e^2/h$ conductance through each point contact
- Dot is well-connected to reservoirs
- Transport measurements exhibit CF and Weak Localization

many open dot slides: A. Huibers and J. Folk

Open Dot Regime: Conductance Fluctuations

$N_L = N_R = 1$

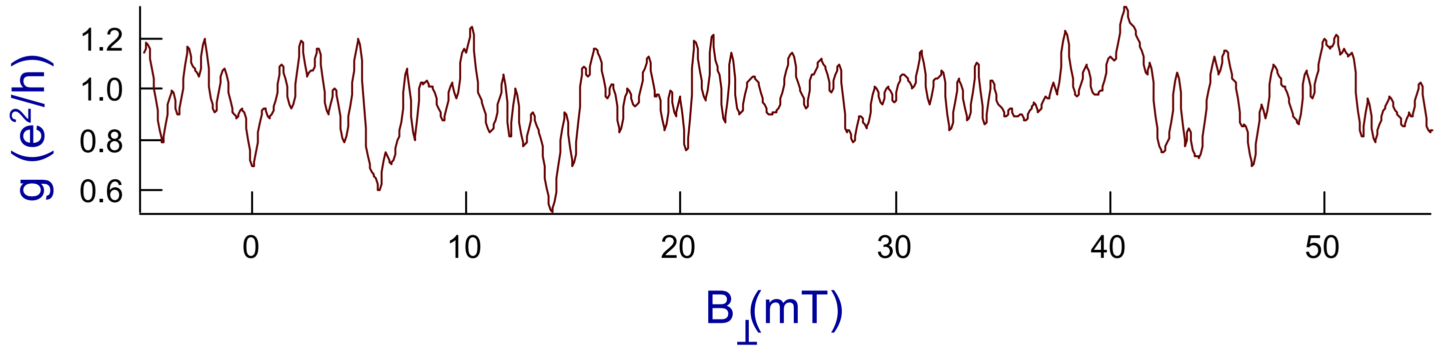

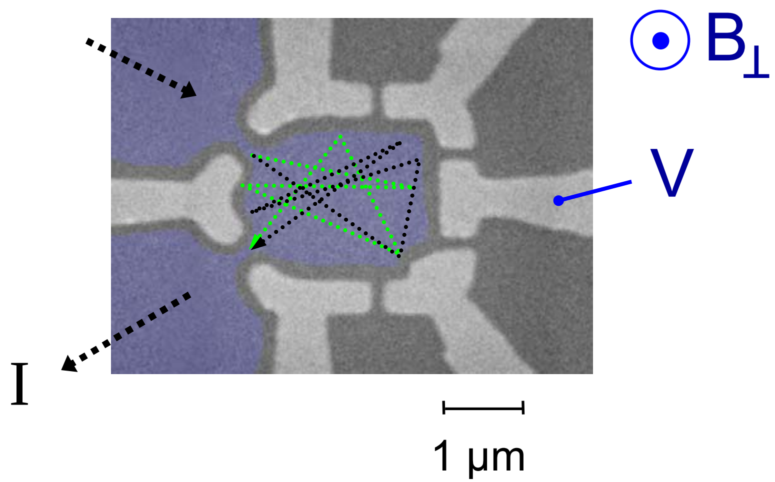

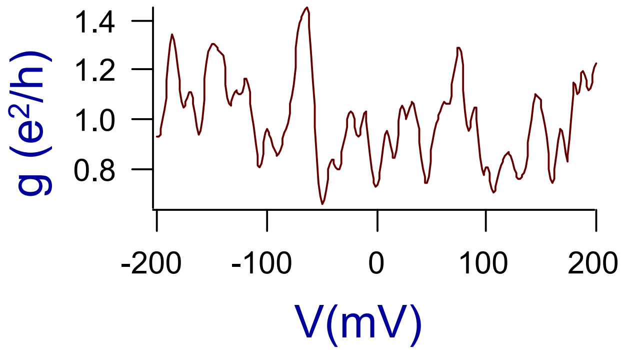

<u>Repeatable</u> random
intereference fluctuations
as function of dot parameters

Two-Dimensional Quantum Dot

2D Cavity with Chaotic trajectories:

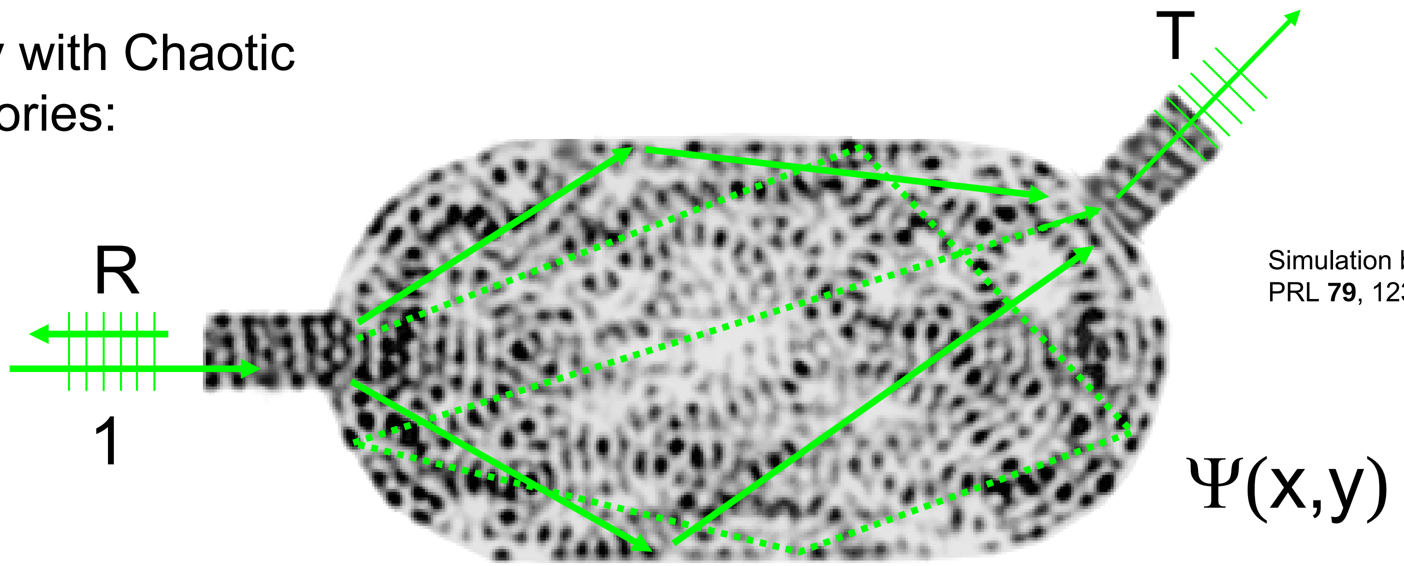

Simulation by R. Akis, PRL **79**, 123 (1997)

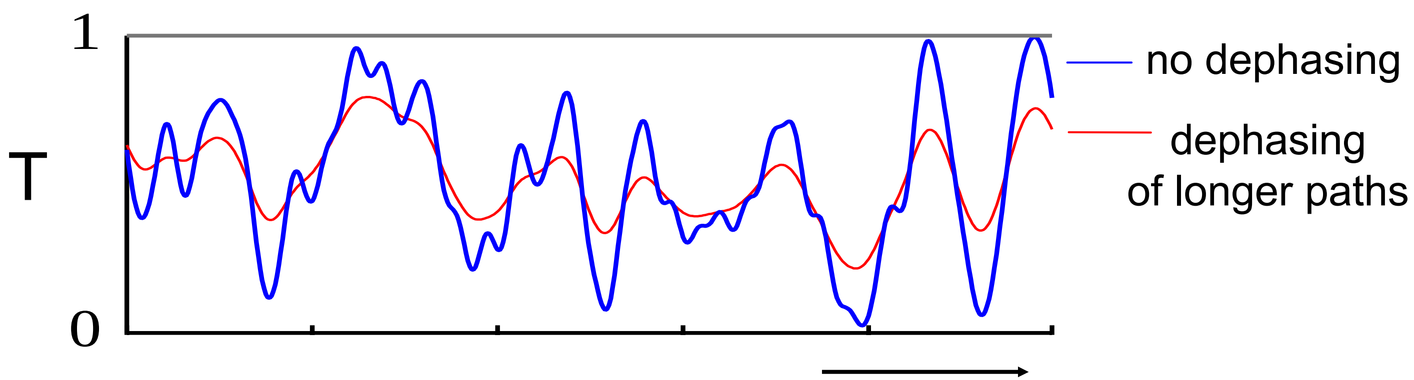

Any parameter that changes path accumulated phase

Goal: use quantum dot as a probe of quantum phase coherence

Interferometers

Two-arm:

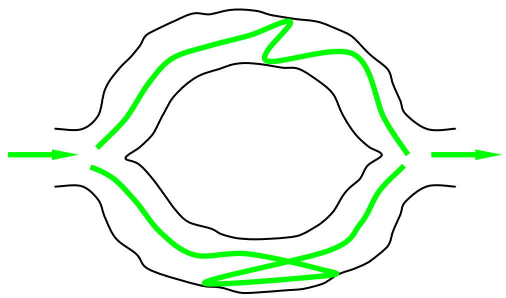

sometimes:
reflections or
small signal

Regular/
Integrable:

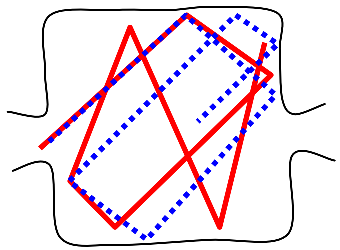

Problem:
partially chaotic

Chaotic:

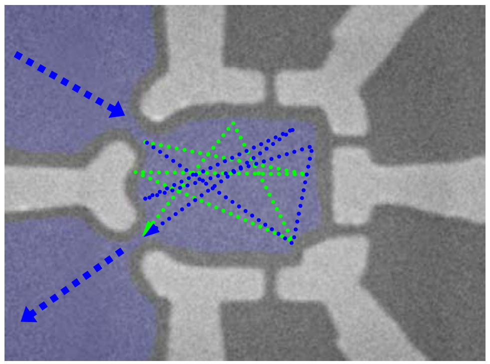

1. Mostly chaotic/ergodic

2. Interesting physics
& complete description

Quantum Interference in Open Dots

Interference between all possible trajectories gives rise to repeatable random intereference fluctuations as function of dot parameters

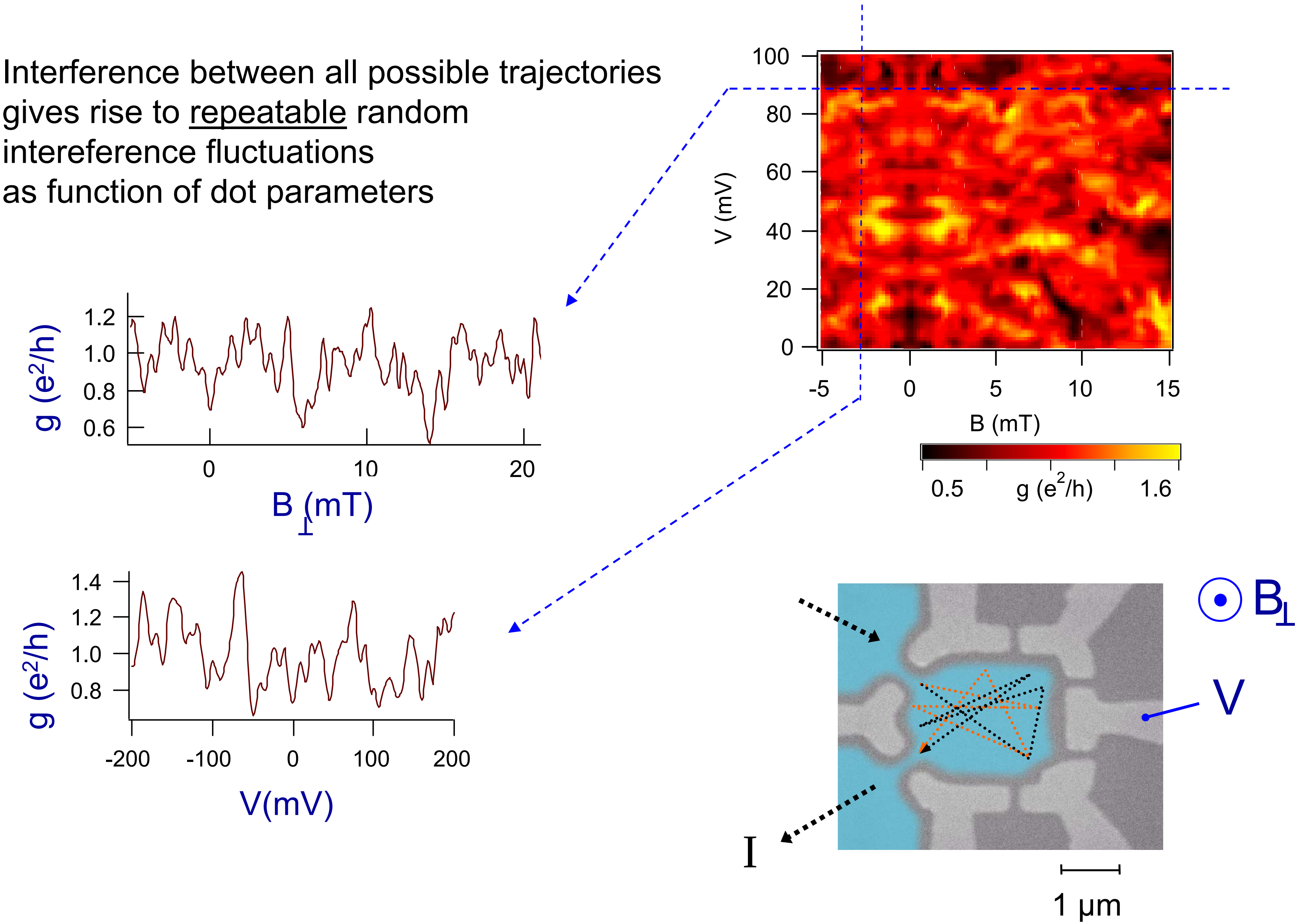

Typical Quantum Dot

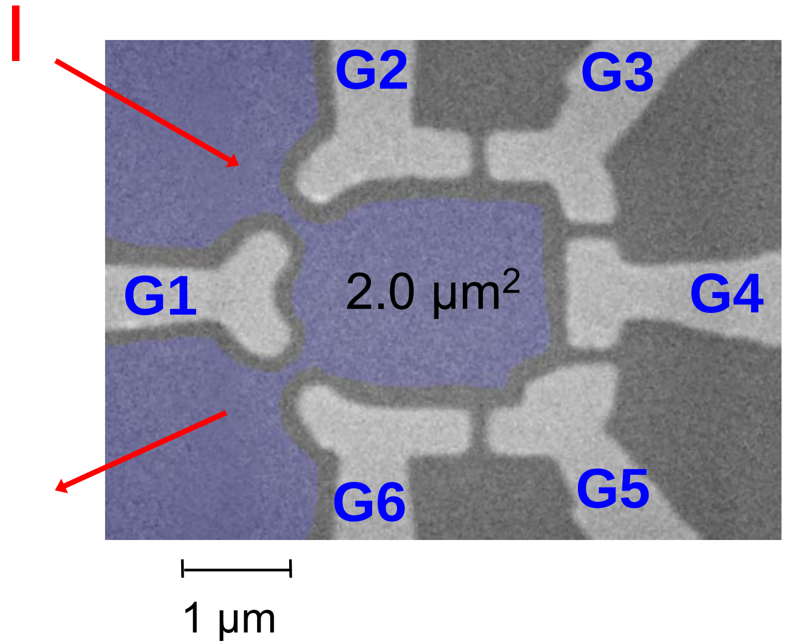

2D conductor:

area = 2.0 μm^2

charge density = 2 10^{11} e/cm^2

λ_F = Fermi wavelength = 50 nm

v_F = Fermi velocity = 200 μm/ns

E_F = Fermi energy = 7 meV

Dwell time in dot:	200 ps
Crossing time:	7 ps
	30 bounces

bulk mean free path ℓ_e ~ 2- 10 μm

Weak Localization

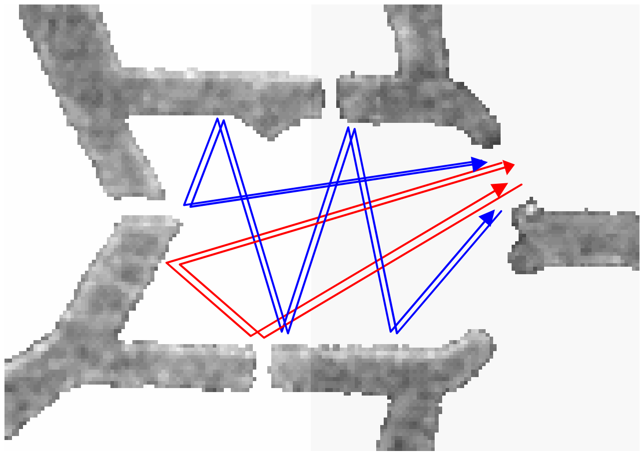

At B=0, phase-coherent backscattering results in “weak localization”

↓

Conductance dip at B=0

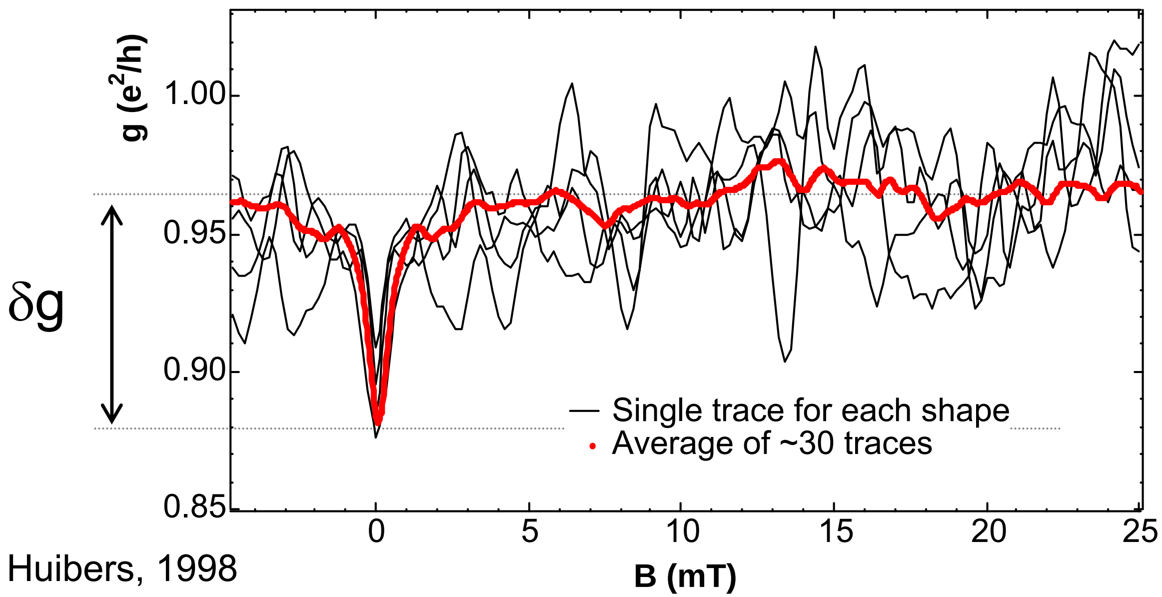

Huibers, 1998

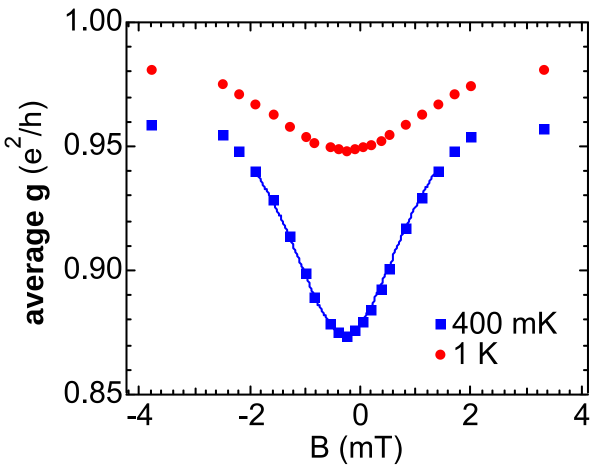

Quantum Correction: Weak Localization

constructive interference of coherently backscattered, time reversed trajectories decreases conductivity

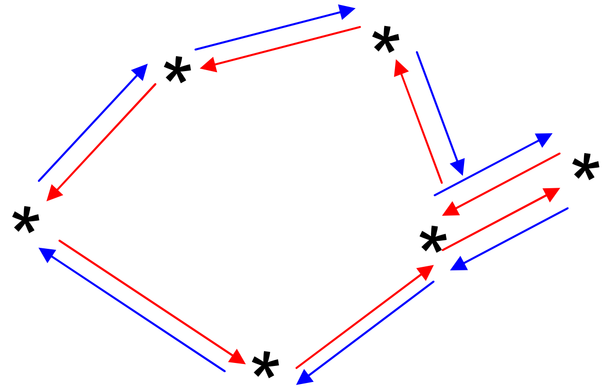

$$\frac{\delta\sigma_{loc}}{\sigma} \propto -\frac{1}{k_F \ell} \ln\left(1+\frac{\tau_\varphi}{\tau}\right) \qquad \text{2D } (L_\varphi << W)$$

$$\frac{\delta\sigma_{loc}}{\sigma} \propto -\frac{L_\varphi}{W}\frac{1}{k_F \ell}\left(1-\left(1+\frac{\tau_\varphi}{\tau}\right)^{-1/2}\right) \qquad \text{1D } (L_\varphi >> W)$$

magnetic field: AB-flux, cut off trajectories of area $A>\phi_0 B$
magnetoconductance

(assuming spinless electrons)

Weak Localization in Magnetic Fields

in a given magnetic field B, trajectories enclosing flux acquire additional Aharonov-Bohm phase:

$$\phi = \frac{2e}{\hbar}\int(\nabla\times A)\cdot d\vec{S} = \frac{2eBS}{\hbar}$$

when summing over all trajectories, this ϕ will effectively eliminate trajectories of area $A >> \phi_0/B$. ($\phi_0 = h/e$)

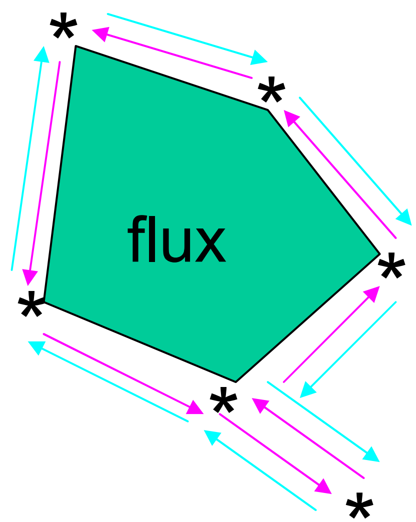

Weak Localization: Measure of Dephasing

1 μm
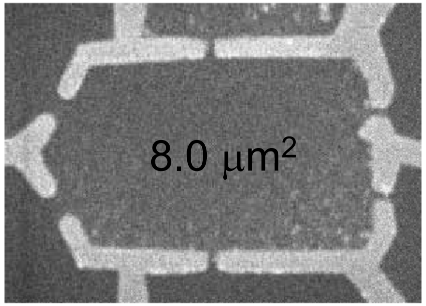

1 μm
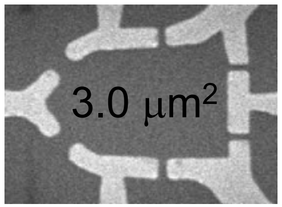

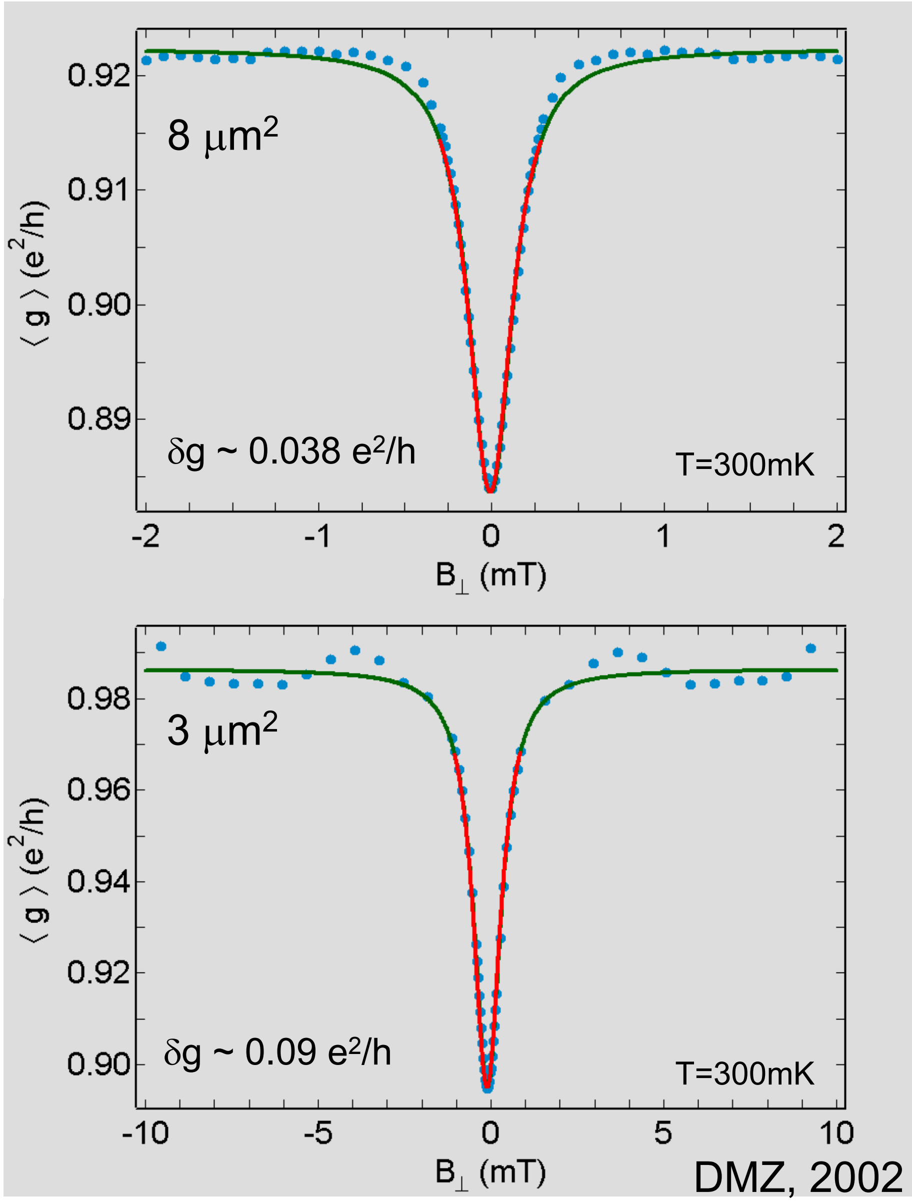

random matrix theory

$$\delta g = \frac{1}{2N + 1 + \gamma_\phi} \qquad \tau_\phi^{-1} = \frac{\Delta}{h} \gamma_\phi$$

Weak Localization vs T

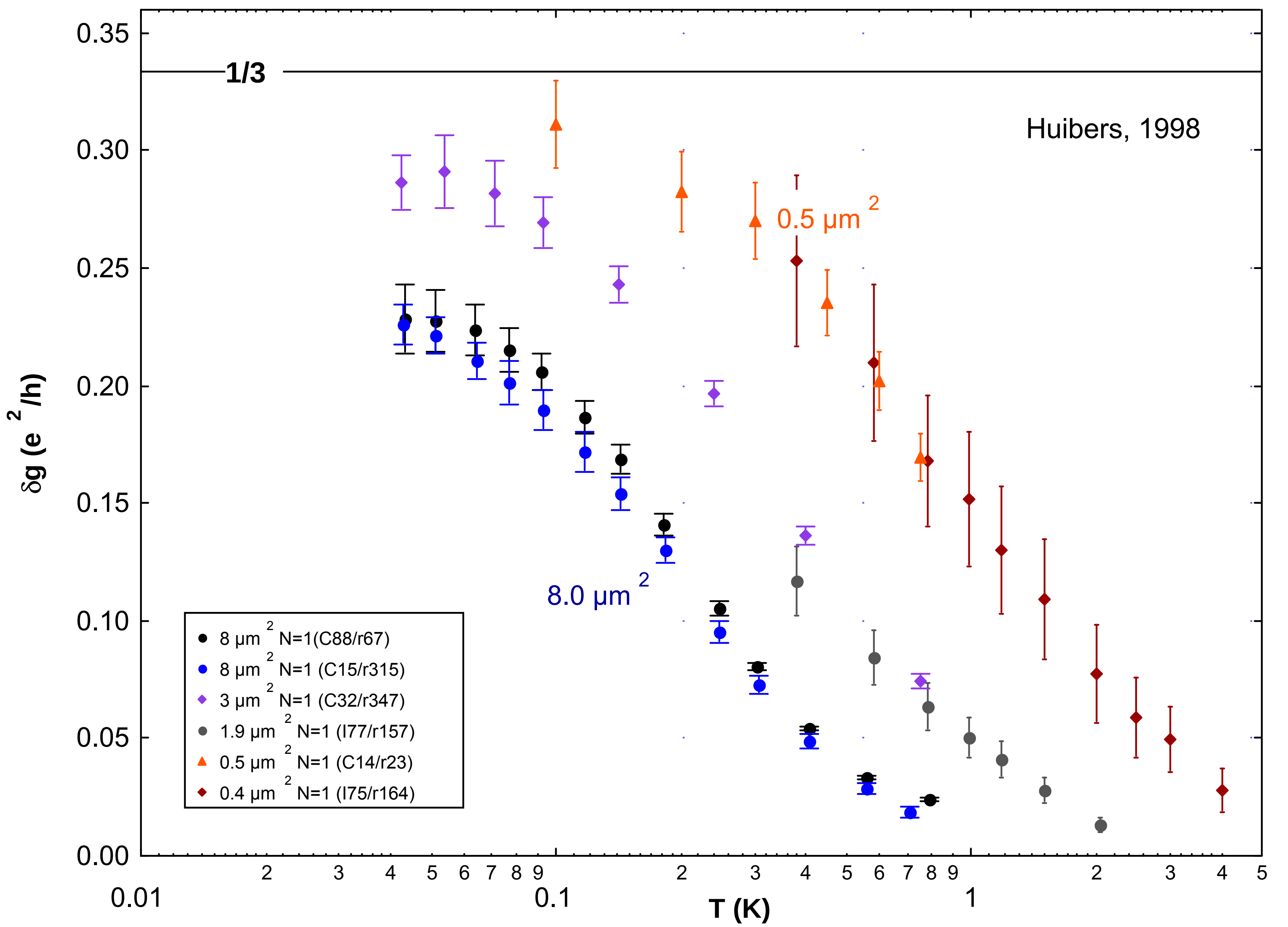

Low Temperature Saturation?

using

$$\delta g = \frac{1}{2N+1+\gamma_\phi}$$

obtain

$$\tau_\phi^{-1} = \frac{\Delta}{h}\gamma_\phi$$

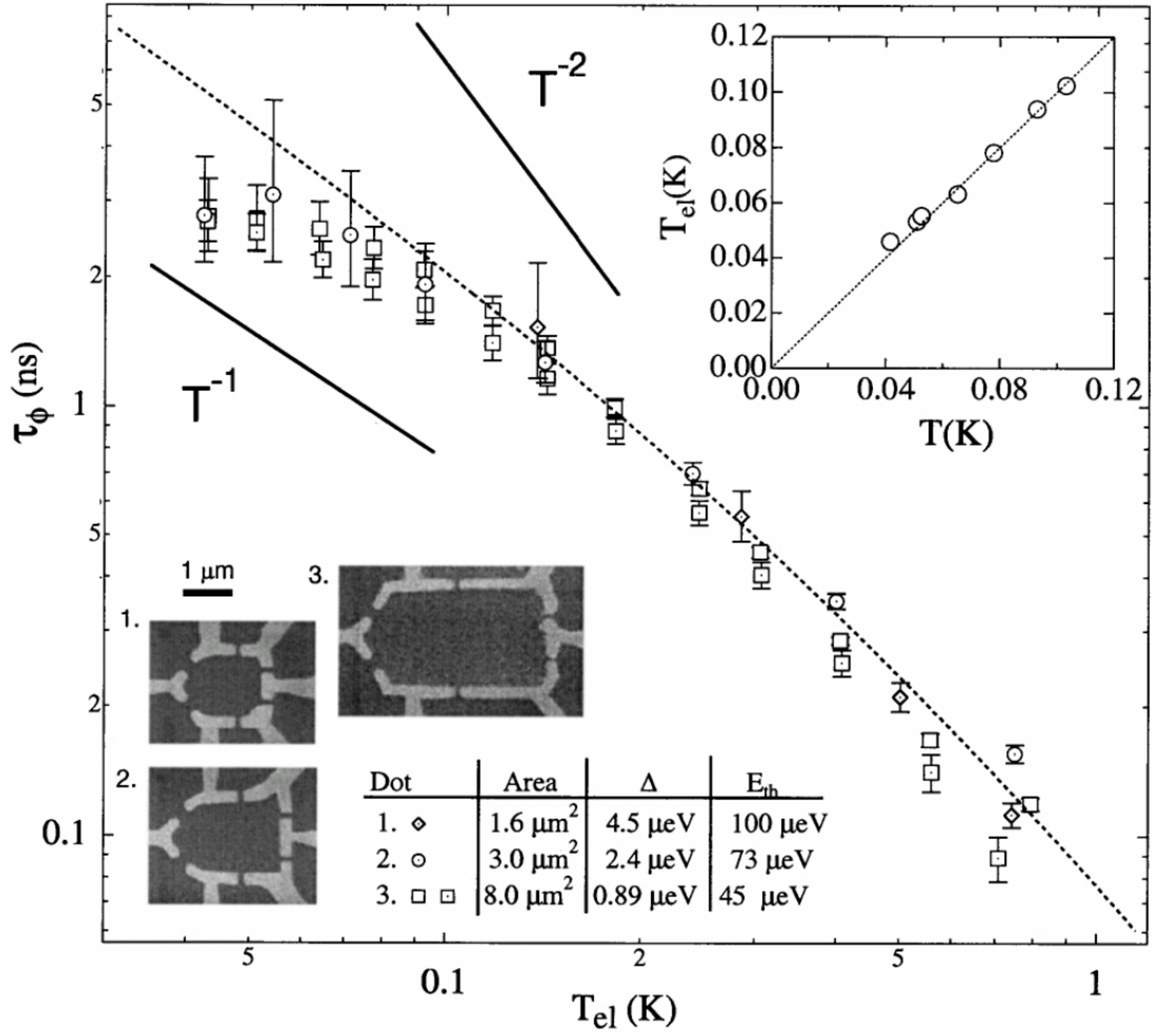

Huibers et al., PRL83, 5090 (1999)

Spin-Orbit Coupling

electrons move with the Fermi velocity, electric fields in material appear as magnetic fields in the rest frame of the electron

these magnetic fields

- depend on magnitude of electron velocity (density dependence)
- couple to the electron spin via Zeeman coupling

→ spin-precessions

electric fields due to:

- heterointerface (***Rashba***)
- crystalline anisotropy in III-V zincblende crystal (***Dresselhaus***)

spin precession affects phase interference
(2π in spin space gives -1 to phase)

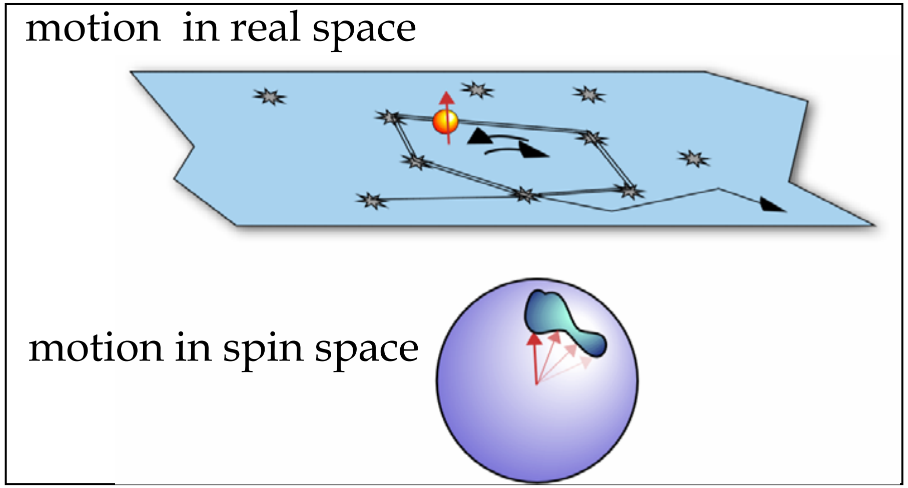

Spin-Orbit Coupling

presence of electric fields $\vec{E} = -\frac{1}{e}\vec{\nabla}V$

electrons are moving in these electric fields

rest frame of electrons: effective magnetic field

$$\vec{B}_{so} = -\frac{\vec{v}}{c} \times \vec{E}$$

magnetic moment $\vec{\mu} = \frac{e\vec{S}}{mc}$ of electron couples to $\vec{B}_{so}$

$$H_{so} = -\vec{\mu} \cdot \vec{B}_{so}$$

electrons precess around B_{so}
B_{so} depends on the electron momentum

spin rotation symmetry is broken,
time reversal symmetry is NOT broken

Spin-Orbit Coupling due to Crystal Anisotropy

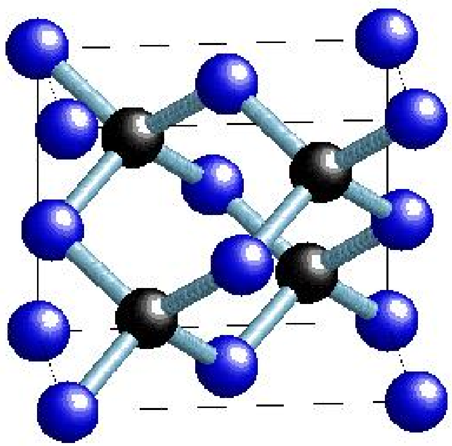

Conventional cell

III-V Semiconductor

Zinkblende crystall structure:
two interpenetrating fcc lattices
with only Ga atoms on one lattice,
only As on the other

absence of inversion symmetry

symmetry considerations:

$$H_{so} = \gamma(\sigma_x k_x (k_y^2 - k_z^2) + \text{cycl.})$$

G. Dresselhaus,
Phys. Rev. 100, 580 (1955)

after size quantization (2D): $\langle k_z \rangle = 0 \qquad \alpha = \gamma \langle k_z^2 \rangle$

$$H_D^{(1)} = \alpha(\sigma_x k_x - \sigma_y k_y)$$ k-linear Dresselhaus term

$$H_D^{(3)} = \gamma(\sigma_y k_y k_x^2 - \sigma_x k_x k_y^2)$$ k-cubic Dresselhaus term

Spin-Orbit Coupling due to Heterointerface

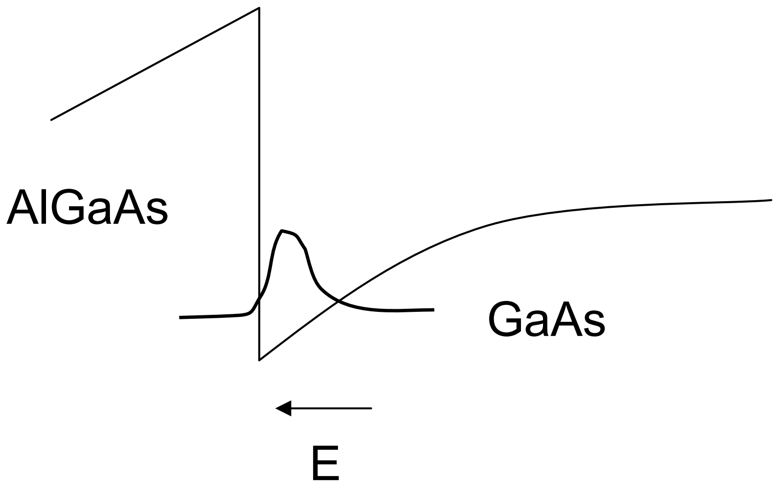

electric field at heterointerface perpendicular to 2D plane

$$\vec{B}_{so} \propto (k_y E, -k_x E, 0) \perp \vec{k}$$

$$H_R = \beta(\sigma_x k_y - \sigma_y k_x)$$ Rashba term (k-linear)

coupling strength parameters β and γ can be determined from Band structure, for example in $k \cdot p$ approximation

Weak Antilocalization

initial state: $|i\rangle$

final (forward): $|f_f\rangle = R_N \ldots R_2 R_1 |i\rangle = R|i\rangle$

final (backward): $|f_b\rangle = R_1^{-1} R_2^{-1} \ldots R_N^{-1} |i\rangle = R^{-1}|i\rangle$ (TRS)

R_i: spin rotations $R = R_N \ldots R_2 R_1$ $R^{\dagger} R = 1$ $R^{-1} = R^{\dagger}$

interference term $\langle f_b | f_f \rangle = \langle i | R^2 | i \rangle$

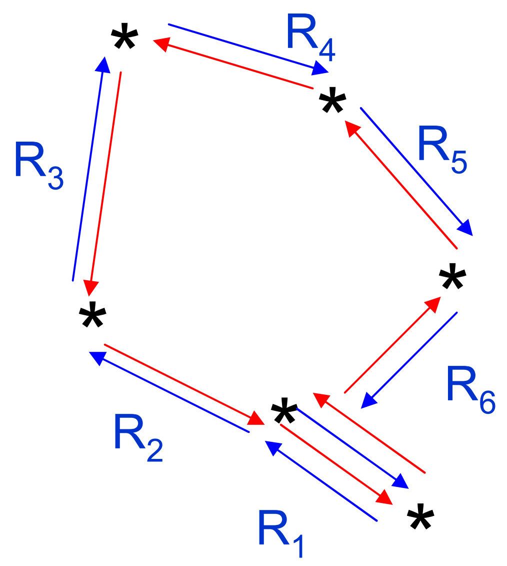

assuming strong spin-orbit coupling,
summing over all trajectories is
equivalent to averaging R^2 over sphere

$$\overline{\langle f_f | f_b \rangle} = -\frac{1}{2}$$

destructive interference
opposite sign for Magnetoconductance

Mechanisms of Spin-Orbit Coupling

Elliott-Yafet

- electric field of atoms/impurities felt during scattering events
- spins precess during scattering events
- spins are invariant between scattering
- spin obrbit spin relaxation time
- dominant mechanism in Au $\tau_{so} \propto \tau_{tr}$

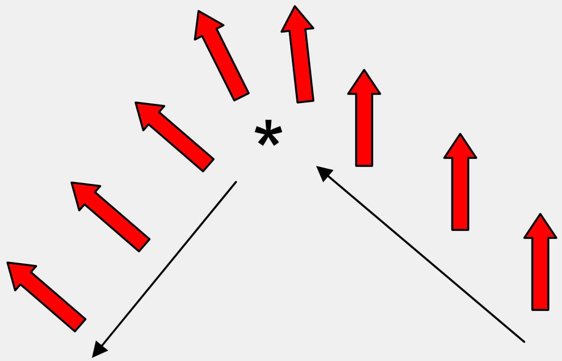

Dyakonov-Perel

- built in electric fields of material
- spin precessions during ballistic travel
- elastic scattering leaves spin invariant
- usually small rotations between scattering assumed, giving a random spin walk, $\tau_{so}^{-1} = \Omega^2 \tau$
- dominant in GaAs heterostructures

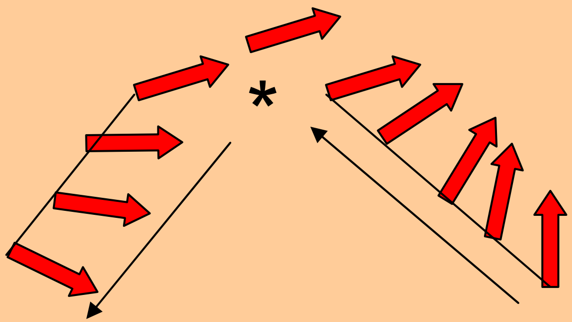

low density
weaker SO coupling
weak localization (WL)

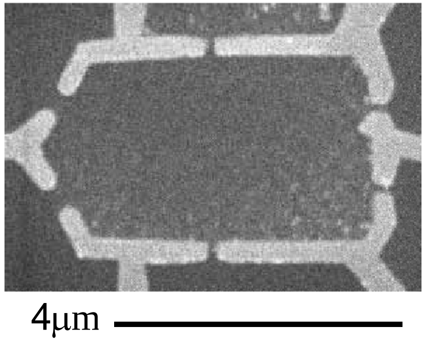

dots are on **different** wafers

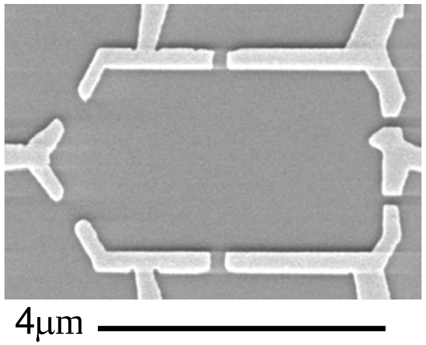

high density
stronger SO coupling
antilocalization (AL)

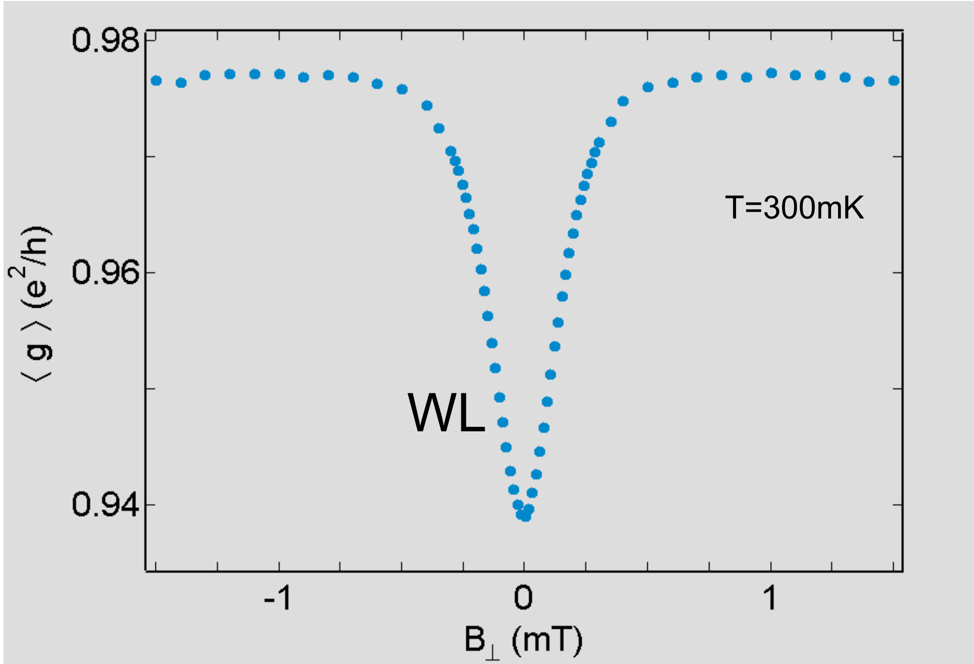

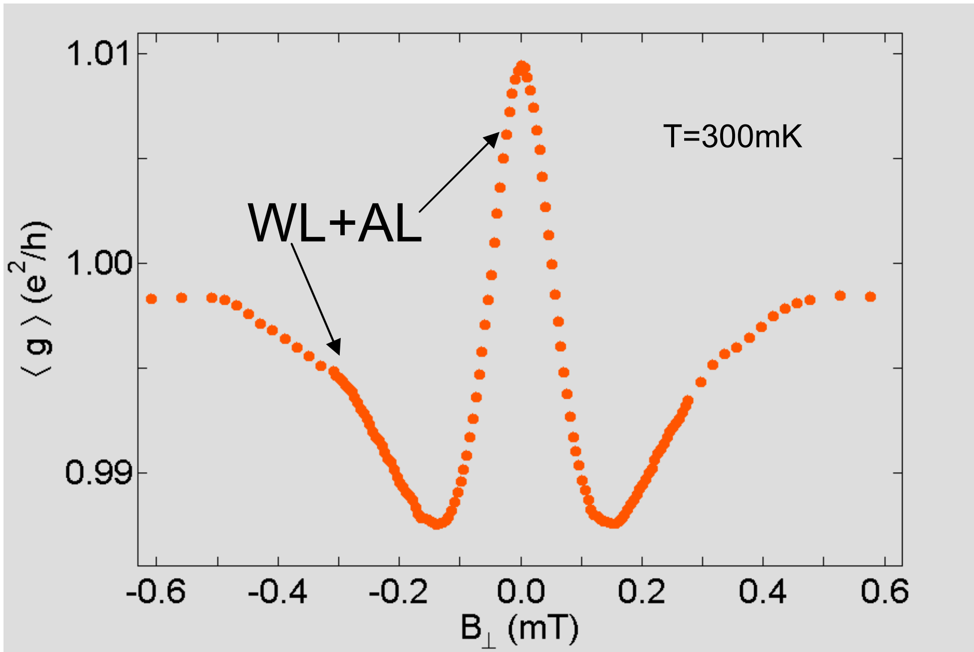

large dot
antilocalization (AL)
due to SO coupling

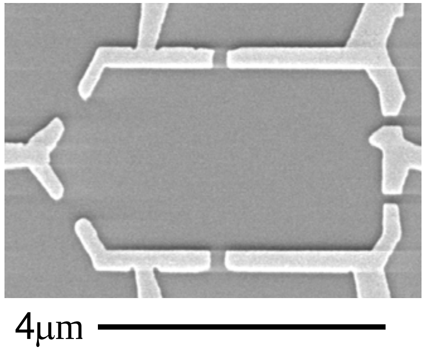

dots on the **same** wafer

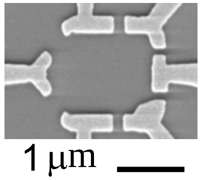

small dot
weak localization (WL)
SO coupling **supressed**

predicted theoretically by:

A. Khaetskii and Y. Nazarov, PRB **61**, 12639 (2000).
B. Halperin et al., PRL **86**, 2106 (2001).
I. Aleiner and V. Fal'ko, PRL **87**, 256801 (2001).

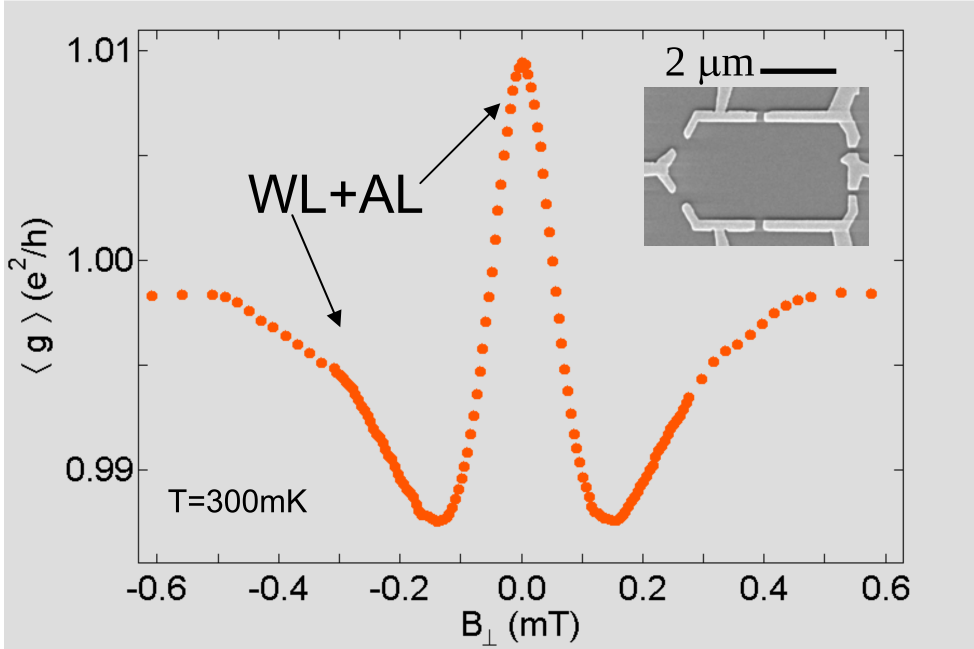

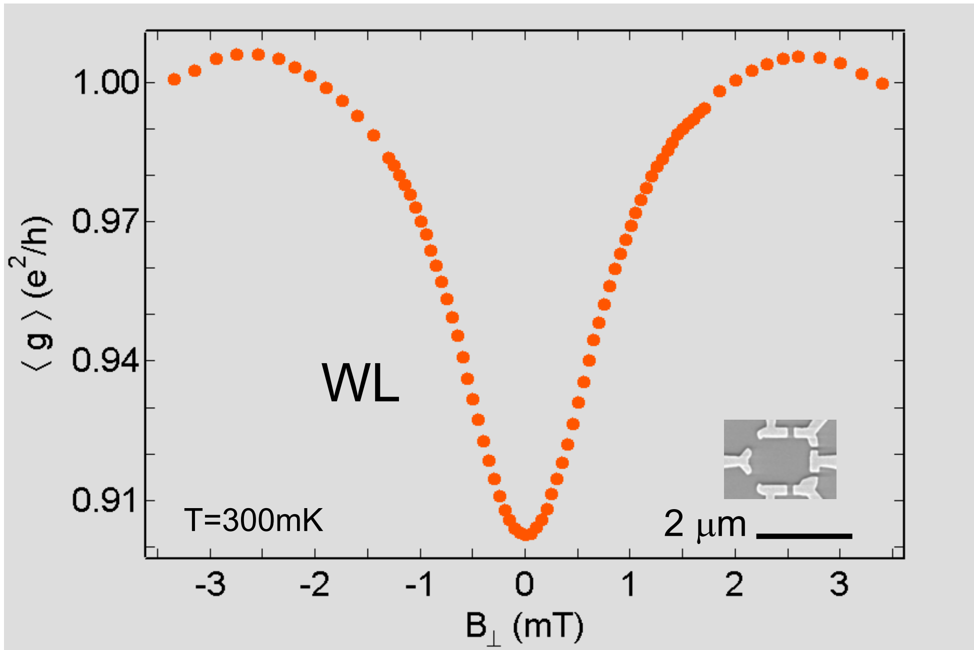

New Random Matrix Theory (SO coupling & $B_{||}$)

$$\langle \delta g \rangle = \frac{e^2}{h}\frac{N}{4}\left\{ -\frac{4b^2 + 2G_C F_C}{\left(4G_C b^2 + G_C^2 F_C - 16a_x^2 F_C x^2\right)} - \frac{4G_C b^2}{F_C\left(4G_C b^2 + G_C^2 F_C - 16a_x^2 F_C x^2\right)} + \frac{4a^2}{F_C\left(4a^2 + F_C\right)} \right\}$$

spin-orbit parameters

$$a_x^2 = \pi\kappa \frac{E_T}{\Delta}\left(\frac{A}{\lambda_1 \lambda_2}\right)^2$$ (AB like SO term)

$$a^2 = \left(\left(\frac{L_1}{\lambda_1}\right)^2 + \left(\frac{L_2}{\lambda_2}\right)^2\right) a_x^2$$ (spin flips)

$$h^2 = \frac{\pi}{2}\left(\frac{E_Z}{\Delta}\right)^2 \left(\frac{\Delta}{E_T}\right)\left(\frac{L}{\lambda_{so}}\right)^2$$ (SO + $B_{||}$)

magnetic fields

$$x^2 = \pi\kappa\left(\frac{E_T}{\Delta}\right)\left(\frac{2eB_\perp A}{h}\right)^2$$ perpendicular

$$b = \pi\frac{g\mu_B B_{||}}{\Delta}$$ parallel

$$N_C = N + 2h^2 + \gamma_\varphi \qquad F_C = N_C + h^2$$

$$G_C = N_C + 2\left(a^2 + a_x^2\right) - h^2$$

λ_1, λ_2	SO length along crystal axes
$\lambda_{so} = \sqrt{\lambda_1 \cdot \lambda_2}$	average SO length
$\nu_{so} = \sqrt{\lambda_1 / \lambda_2}$	SO anisotropy
γ_φ	decoherence rate
κ	geometry dependent constant

Jan-Hein Cremers, Piet Brouwer, Vladimir Fal'ko, Phys. Rev. B**68**, 125329 (2003)

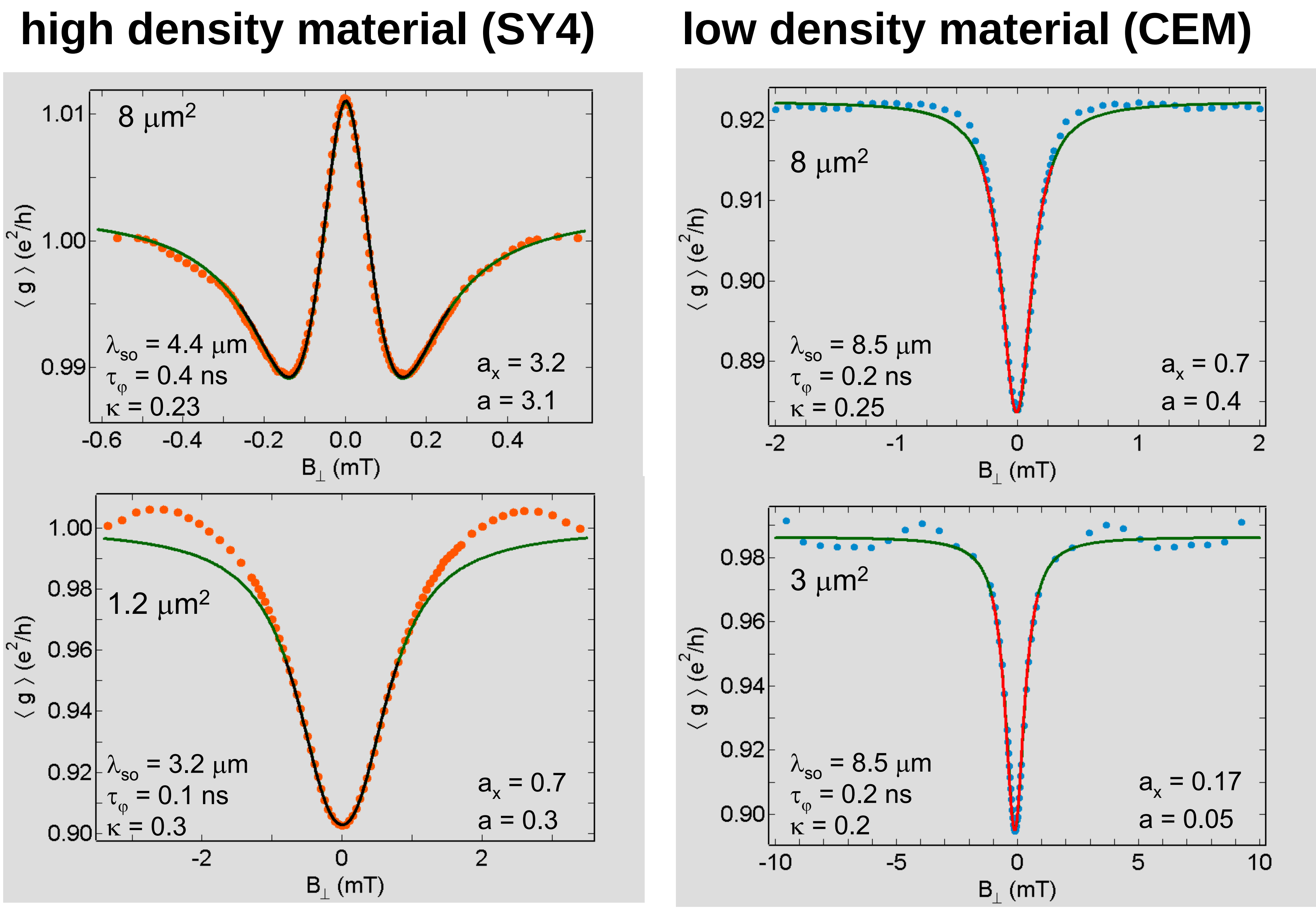

high density material (SY4)
low density material (CEM)
8 μm²
λso = 4.4 μm
τφ = 0.4 ns
κ = 0.23
ax = 3.2
a = 3.1
1.2 μm²
λso = 3.2 μm
τφ = 0.1 ns
κ = 0.3
ax = 0.7
a = 0.3
8 μm²
λso = 8.5 μm
τφ = 0.2 ns
κ = 0.25
ax = 0.7
a = 0.4
3 μm²
λso = 8.5 μm
τφ = 0.2 ns
κ = 0.2
ax = 0.17
a = 0.05
⟨ g ⟩ (e²/h)
B⊥ (mT)

Suppression of Spin-Orbit Coupling in Dots

$\lambda_{so} \sim L$

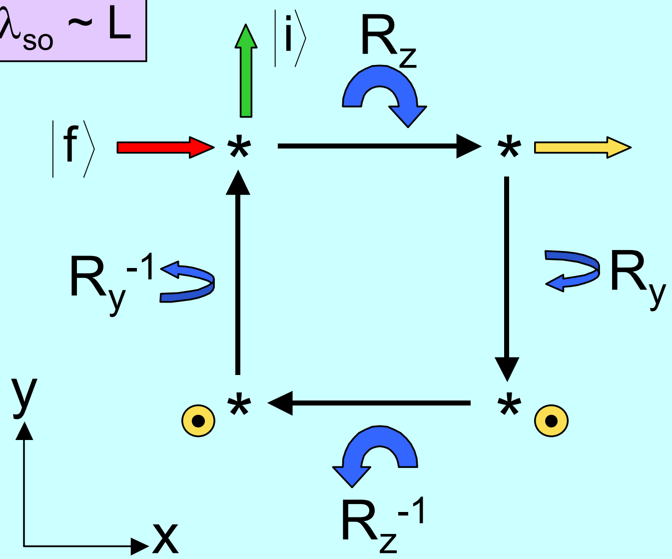

$$|f\rangle = R_y^{-1} R_z^{-1} R_y R_z |i\rangle \neq |i\rangle$$

large rotations,
order of rotations matter

$\lambda_{so} \gg L$

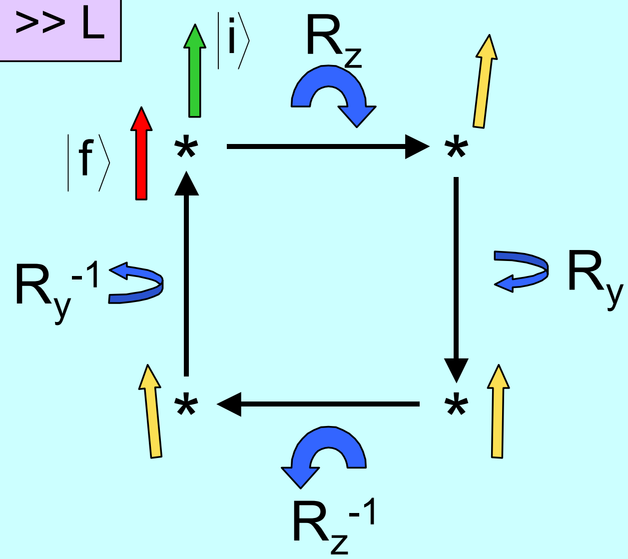

$$|f\rangle = R_y^{-1} R_z^{-1} R_y R_z |i\rangle$$

$$\approx R_y^{-1} R_y R_z^{-1} R_z |i\rangle = |i\rangle$$

small rotations,
commute, cancelation